

ANALYSIS OF NUCLIDE TRANSPORT INCLUDING NON-LINEAR ADSORPTION DEPENDING ON VARIABLE SALINITY IN THE HETEROGENEOUS GEOSPHERE OF THE GORLEBEN CHANNEL

Vijen Javeri

Gesellschaft für Anlagen- und Reaktorsicherheit (GRS) mbH
Schwertnergasse 1, 50667 Cologne, Germany
e-mail: jav@grs.de

ABSTRACT

After studying the two and three dimensional Elder-Problem, the impacts of variable salinity or liquid density and of non-linear adsorption on the nuclide transport in the heterogeneous geosphere above the salt dome of the Gorleben channel are investigated using the computer code TOUGH2/EOS7R, which is modified to simulate permeability depending upon volume element, non-linear nuclide adsorption depending upon nuclide and brine mass fraction, etc. A detailed two dimensional model with more than 13700 volume elements and with several highly space dependent hydrogeological units is employed. The analysis including four liquid components (groundwater, denser brine, parent nuclide, daughter nuclide) shows: With increasing salinity a recirculating flow can be established, which can reduce the nuclide transport substantially; with increasing salinity nuclide advection and also adsorption are reduced.

INTRODUCTION

To assess the long-term safety of a repository for the radioactive waste in a deep salt rock formation, generally, a brine inflow into the repository is postulated. After being dissolved in brine the nuclides can be transported out of the repository and subsequently can be released into geosphere. The liquid density and viscosity depend on salinity, as the liquid phase consists of denser contaminated brine emerging from the underlying salt area and of lighter groundwater. After studying the two and three dimensional Elder-Problem, the impacts of variable salinity or liquid density and non-linear adsorption on the nuclide transport in the heterogeneous geosphere above the salt dome of the Gorleben channel are investigated within a scoping analysis using the code TOUGH2/EOS7R, which is modified to simulate: (a) permeability and porosity depending on volume element, (b) sources of brine, parent nuclide and daughter nuclide in the same volume element, (c) non-linear nuclide adsorption depending on nuclide and brine mass fraction, (d) boundary condition of the third kind for the inflow of contaminated brine.

MODIFICATION OF TOUGH2 MODELS

Originally in TOUGH2/EOS7R (Pruess 1991, 1995), the nuclide adsorption on a solid surface is described by the linear Henry function:

$$C_i = \rho_F X_i, \quad Y_{\text{Ads},i} = K_{d,i} C_i.$$

To consider non-linear adsorption according to the Langmuir or Freundlich function and to include the influence of salinity, TOUGH2/EOS7R is extended as follows (Javeri 2000):

$$Y_{\text{Langmuir,Ads},i} = [K_{L,i} C_i / (1 + L_{L,i} C_i)] f_{\text{salt},i}(X_2),$$

$$Y_{\text{Freundlich,Ads},i} = K_{F,i} C_i^b f_{\text{salt},i}(X_2), \quad X_2 = m_2/m_F,$$

K_L : Langmuir distribution coefficient,
 K_F : Freundlich distribution coefficient,
 L_L : Langmuir parameter,
 b_i : Freundlich exponent.

The Langmuir parameters K_L , L_L , the Freundlich parameters K_F , b and the arbitrary function f_{salt} , which are to be defined by the user for a problem given, depend upon nuclide and rock type.

In the original version of TOUGH2/EOS7R, a source of only one component in a volume element is allowed. To include sources of more than one component in the same element and to simulate approximately the boundary condition of the third kind (source or flux $\sim \text{grad } X$) at the bottom boundary, TOUGH2/EOS7R is extended to treat two and three dimensional configuration (Javeri 2001):

$$Q_2(X_2) = Q_{2,0} (X_{2,\text{ambient}} - X_2), \quad Q_3 = a_3(t) Q_2(X_2),$$

$$Q_{2,0} = n d \rho_F A / (\Delta z/2), \quad Q_4 = a_4(t) Q_2(X_2),$$

$a_3(t)$ and $a_4(t)$: functions to be defined by the user.

TWO AND THREE DIMENSIONAL ELDER PROBLEM

Before performing two dimensional analysis of nuclide transport including non-linear adsorption depending on variable salinity, two and three

dimensional isothermal natural convection caused by variable liquid density as defined by the well known Elder problem are studied to estimate the influence of the boundary condition on the fingering of brine concentration. Assuming $1/\rho_F = (1-X_2)/\rho_1 + X_2/\rho_2$, two and three dimensional cases utilizing the symmetry of the problem are considered (Fig. 1):

Case EP1: This frequently studied two dimensional problem can be derived from the three dimensional symmetrical problem as analysed in (Diersch 1998), if a unit width in the y-direction is postulated and if the y-dependence is neglected. A uniform mesh of 1800 equal volume elements with $\Delta x = \Delta z = 5$ m is used for the horizontal length of 300 m and for the vertical height of 150 m. The upper boundary condition of pure brine at $z = 0$ holds only for $0 \leq x \leq 150$ m.

Case EP25: as EP1, but the top boundary condition of pure brine at $z = 0$ holds only for $0 \leq x \leq 75$ m.

Case DEP1F: In this three dimensional problem, the horizontal length of 300 m in x- and y-direction is discretized by 50 equal elements of 6 m in both directions and the vertical height of 150 m in z-direction by 30 equal elements of 5 m. The total number of elements amounts to be 75000. The upper boundary condition of pure brine at $z = 0$ holds only for $0 \leq x \leq 150$ m and $0 \leq y \leq 150$ m.

Case DEP2F: as DEP1F, but the top boundary surface with pure brine is extended roughly by a factor of two; this boundary condition of pure brine at $z = 0$ holds only for $0 \leq x \leq 216$ m and $0 \leq y \leq 216$ m or for 36 elements in both horizontal directions.

These four cases are computed using TOUGH2/EOS7 with a maximum time step of 4E6 sec. Depending upon the case, the steady state is reached between 150 and 250 years. To clarify the influence of discretisation, the base case EP1 was repeated with finer meshes: Case EP1F: 7200 uniform elements of 2.5 m in both directions; Case EP1FF: 20000 uniform elements of 1.5 m in both directions. The cases EP1, EP1F and EP1FF showed practically the same brine distribution. In Fig. 2 to 5 the steady state brine mass fractions and flow directions depicted for the selected y-planes in the different cases. The results of the base case EP1, specially the fingering and the upward flow along the axis of symmetry and along the outer boundaries, are in good agreement with (Oldenburg 1997, Diersch 1998). Fig. 6 and 7 show the steady state brine distribution at $z = -12.5$ m near the top surface in three dimensional cases DEP1F and DEP2F; as expected, the distributions are exactly symmetrical with respect to the diagonal connecting $x = y = 0$ and $x = y = 300$ m. Unfortunately, the present steady state results of the three dimensional cases cannot be

compared with (Diersch 1998), as they published the results for twenty years only. The present results of convection in a two or three dimensional Elder-type system suggest that the steady state fingering of brine concentration with more than one convection cell in one half plane of the symmetrical system is to be expected, if $A_{in}/A_{out} = (\text{in-diffusion area at the top}) / (\text{out-diffusion area at the bottom}) \geq 1/2$. In the two dimensional case EP25 and in the three dimensional case DEP1F with $A_{in}/A_{out} = 1/4$, the steady state fingering is not observed; but in the cases EP1 and DEP2F with $A_{in}/A_{out} \geq 1/2$ it does occur. Several calculations on thermohaline convection indicate that TOUGH2 can yield stable converging results, if the mesh Peclet-number $Pe = u\Delta x / (nd) \leq 4$ and Courant-number $Co = u\Delta t / (nR\Delta x) \leq 2$ (Javeri 1999).

NUCLIDE TRANSPORT DEPENDING ON SALINITY

To analyze the nuclide transport considering variable liquid density and non-linear adsorption depending upon salinity in the geosphere above the salt dome of the Gorleben channel, a detailed two dimensional model with highly space dependent anisotropic hydrological parameters is employed (Fig. 8). The distributions of the porosity (between 5 and 26 %) and the horizontal permeability (between $1E-17$ and $1E-11$ m²) for the total of 13729 volume elements were sampled by geostatistical methods using available borehole data separately prior to transport analysis and are simulated by 20 different clay and non-clay rock types in TOUGH2 calculations. The vertical permeability of 20 rock types is only 1/10 of the corresponding horizontal value.

In the present model (Fig. 8), following a prescribed horizontal pressure gradient on the top boundary, groundwater enters from the top boundary on the left side, flows through a region with a transient source of contaminated dense brine with an arbitrary parent and a daughter nuclide at the bottom, and then flows out at the top and at the right boundary. In domain 4 in the bottom region, a source of contaminated brine emerging from a postulated repository in the underlying salt formation is introduced. To limit the computational efforts, the dispersion is neglected; the brine and the nuclides are transported by advection and diffusion only. However, the possible dispersion effects can be enveloped by appropriate diffusion coefficients reasonably (Javeri 2002). The fictitious nuclides have the same molecular weight and do not influence the liquid properties. The important parameters and the cases considered are:

$$\rho_1 = \rho_{\text{water}}(p, T), \quad \rho_{\text{rock}} = 1900 \text{ kg/m}^3,$$

$$\rho_2(p = 1 \text{ bar}, T = 25 \text{ C}) = 1200 \text{ kg/m}^3,$$

$1/\rho_F = (1-X_2)/\rho_1 + X_2/\rho_2$, $d = 1E-7 \text{ m}^2$,
 $\mu_F = \mu_{\text{water}}(p,T) [1+0.4819X_2+0.2774X_2^2+0.7814X_2^3]$,
 half-life of parent nuclide: 5000 years,
 half-life of daughter nuclide: 10000 years,
 domain 4: $x = 2640$ to 3140 m , $\Delta z = 10 \text{ m}$,

$$n = 0.26, k_{\text{hor}} = 4E-12 \text{ m}^2, k_{\text{ver}} = k_{\text{hor}}/10,$$

$$X_{2,\text{ambient}} = 1, a_3(t) = 0.01, a_4(t) = 0.001,$$

$$Q_{2,0} = (0.26)(1E-7)(1200)(500)/5,$$

$$Q_{2,0} = 0.00312 \text{ kg/s or } 98392 \text{ kg/year},$$

$$Q_2 = Q_{2,0} (1 - X_2),$$

$$Q_3 = Q_2/100, Q_4 = Q_2/1000,$$

initial condition : only groundwater, steady state pressure distribution, $X_1 = 1$, $T = 25 \text{ C}$,

boundary conditions :

left and bottom : impermeable,
 right: only groundwater, $T = 25 \text{ C}$, $p = p(z)$,
 no diffusion, horizontal advection only,
 top: only groundwater, $T = 25 \text{ C}$,
 horizontal grad $p = 6.24 \text{ Pa/m}$,
 no diffusion, vertical advection only.

Case GP1: no nuclide adsorption.

Case GP1K: as GP1, but $\rho_1 = \rho_2 = \rho_{\text{water}}$,
 $Q_{2,0} = 81194 \text{ kg/year}$.

Case GP1A: as GP1, but with Freundlich adsorption independent of salinity outside domain 4:
 parent nuclide: $K_{F,3} = 0.0002 \text{ m}^3/\text{kg}$, $b_3 = 0.8$,
 daughter nuclide: $K_{F,4} = 0.0005 \text{ m}^3/\text{kg}$, $b_4 = 0.9$,
 $f_{\text{salt},3} = f_{\text{salt},4} = 1$.

Case GP1AS: as GP1A, but the nuclide adsorption depends upon brine fraction outside domain 4. For a real geological formation, the function f_{salt} depends on the geochemical properties of the liquid phase and hence it should be derived from the appropriate geochemical experiments. However, for the present scoping analysis with fictitious nuclides, a simple exponential function is postulated, which describes qualitatively the experimental observations indicating that with increasing salinity, the adsorption of heavy metal ions are reduced up to a factor of 100 (Baltes et al 1998, chapter 2.4.3). The case GP1AS is like GP1A, but $f_{\text{salt},3} = f_{\text{salt},4} = \exp(-5X_2)$.

Case GP1H: as GP1, but the logarithmic mean values for porosity and permeability are derived from all volume elements j to simulate a homogeneous geosphere with constant properties in the total region:

$$V_{\text{total}} \log(n_{\text{mean}}) = \sum V_j \log(n_j), \quad n_{\text{mean}} = 0.179,$$

$$V_{\text{total}} \log(k_{\text{hor, mean}}) = \sum V_j \log(k_{\text{hor},j}),$$

$$k_{\text{hor, mean}} = 2.36E-13 \text{ m}^2, \quad k_{\text{ver, mean}} = 2.36E-14 \text{ m}^2.$$

These cases are computed with the modified TOUGH2/EOS7 considering four liquid components (groundwater, brine, parent nuclide, daughter nuclide), variable liquid density and non-linear nuclide adsorption depending upon salinity, until the steady state is reached. Fig. 9 shows the steady state brine mass fraction in liquid phase and pore velocity for the case GP1. Their distributions are governed by the differently influencing effects: the prescribed pressure gradient on the top boundary generates main flow from left to right, the diffusion acts equally in all directions and the density gradient moves denser liquid from top to bottom and the lighter liquid from bottom to top. All these effects can lead finally to a recirculating flow and to a significant brine mass fraction in the lower region delaying the nuclide transport away from the source. Fig. 10 shows the source and the total outflow of brine in case GP1 with heterogeneous geosphere and in case GP1H with homogeneous geosphere and indicates clearly that the steady state is reached. As the nuclides do not influence the liquid density, the source and the outflow of brine are same in case GP1, GP1A and GP1AS. Since the pathways of higher permeabilities in case GP1H are missing, the salinity in the bottom region is higher and hence the source of the contaminated brine is less than in case GP1. The homogeneity in case GP1H does not produce an outward flow at the top boundary; the brine and the nuclides are released only at the right boundary. For an integral comparison, the outflows of brine and nuclides at the top and at the right boundary are depicted in Fig. 11 to 15. In case GP1K with density independent of salinity, the outflows of brine and nuclides at the top boundary are higher than in case GP1 with denser liquid stratifying in the lower region. By the same token, the outflows at the right boundary in case GP1 are higher than in case GP1K. Due to adsorption, the nuclide fluxes at the boundaries in case GP1A are lower than in case GP1. But the reduced adsorption due to salinity in case GP1AS leads to a higher nuclide outflow than in case GP1A. Additional calculations considering dispersion and different boundary conditions indicate that the possible dispersion effects can reasonably be enveloped by appropriate diffusion coefficients (Javeri 2002).

CONCLUSION

The results regarding natural convection in a two or three dimensional Elder-type configuration suggest that the steady state fingering of brine concentration with more than one convection cell in one half plane of the symmetrical system is to be expected, if

(in-diffusion area at the top) / (out-diffusion area at the bottom) $\geq 1/2$.

Summarizing one can conclude from several two and three dimensional scoping analyses on nuclide transport considering variable salinity, non-linear adsorption and different boundary conditions:

(a) With increasing brine fraction, a recirculating flow can occur, which can reduce the nuclide transport substantially.

(b) The nuclide adsorption depending upon salinity can influence the nuclide distribution and can reduce the nuclide retention significantly; with increasing salinity the nuclide advection and also the nuclide adsorption are reduced.

(c) Depending upon the salinity, the problem specifications and the boundary conditions applied, the heterogeneity of a porous medium can enhance the vertical nuclide transport substantially compared to a homogeneous porous medium with an estimated equivalent permeability and porosity.

SYMBOLS

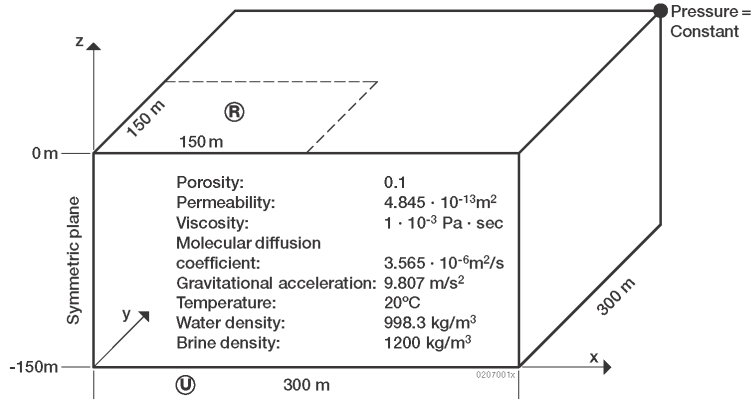
A : area [m²]
C : concentration [kg/m³]
K : distribution coefficient [m³/kg]
Q : source [kg/sec]
R : retardation factor
T : temperature [grad C]
V : volume [m³]
X : mass fraction in liquid phase
Y : mass fraction in solid phase
a : arbitrary function
d : molecular diffusion coefficient [m²/s]
k : permeability [m²]
m : mass [kg]
n : porosity
t : time [s]
u : Darcy velocity [m/s]
 μ : dynamic viscosity [Pa sec]
 ρ : density [kg/m³]

SUBSCRIPTS

F : liquid phase
i : liquid component 1 to 4 (1: groundwater,
2: saturated brine, 3: parent nuclide,
4: daughter nuclide)

REFERENCES

- Baltes, B. et al, GRS-Report GRS-A-140/2, Cologne, Germany, June 1998.
- Diersch, H. et al, Coupled groundwater flow and transport: 2. Thermohaline and 3d convection systems, *Advances in water resources*, 21, 401- 425, April 1998.
- Javeri, V., *Analysen zur thermohaline Konvektion in einem heterogenen porösen Medium mit dem Rechenprogramm TOUGH2*, GRS-A-2697 [BMU-2001-578], May 1999.
- Javeri, V., *Analysis of nuclide transport including non-linear adsorption depending on brine fraction in a two dimensional heterogeneous porous medium*, Int. Conf. on Radioactive Waste Disposal, Distec 2000, 459 – 464, Berlin, September 2000.
- Javeri, V., *Dreidimensionale Analysen zum Nuklidtransport bei salzanteilabhängiger Adsorption in einem porösen Medium mit dem Rechenprogramm TOUGH2*, GRS-A-2864 [BMU-2001-584], March 2001.
- Javeri, V., GRS-Reports GRS-A-3008, February 2002 and GRS-A-3038, August 2002 [restricted distribution].
- Oldenburg, C. et al, Dispersive transport dynamics in a strongly coupled groundwater-brine flow system, *Water Resources Research*, 31, 289 – 302, February 1995.
- Pruess, K., *TOUGH2-A general purpose numerical simulator for multiphase fluid and heat flow*, LBL-29400, May 1991 and *EOS7: An equation of state module for the TOUGH2 simulator for two phase flow saline water and air*, LBL-31114, Lawrence Berkeley Laboratory, Berkeley, California, August 1991.
- Pruess, K., *EOS7R: Radionuclide transport for TOUGH2*, LBL-34868, Lawrence Berkeley Laboratory, Berkeley, California, November 1995.



Plane $x = 0$ and plane $y = 0$: Symmetric plane
 Boundary condition \textcircled{R} : $x = 0$ to 150 m ; $y = 0$ to 150 m ; $z = 0$; pure brine; only diffusion
 Boundary condition \textcircled{U} : $x = 0$ to 300 m ; $y = 0$ to 300 m ; $z = -150 \text{ m}$; pure water; only diffusion
 All boundary surfaces: impermeable
 Initial condition: no salinity, steady state pressure distribution

Figure 1. Three –dimensional Elder problem

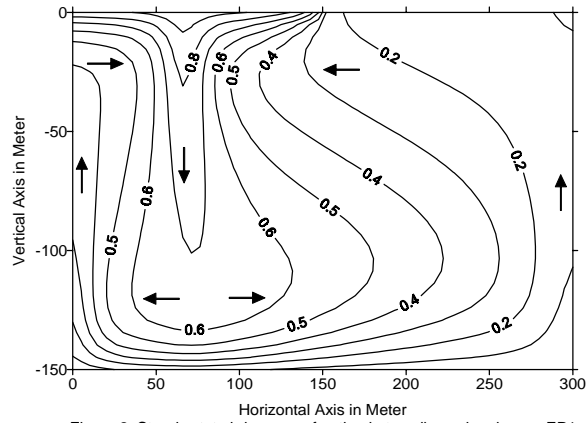


Figure 2. Steady state brine mass fraction in two-dimensional case EP1

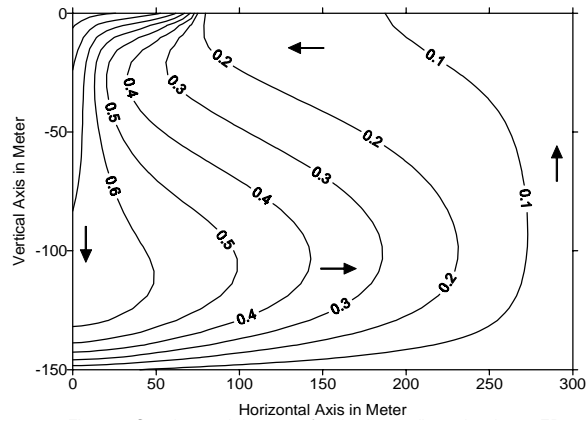


Figure 3. Steady state brine mass fraction in two-dimensional case EP25

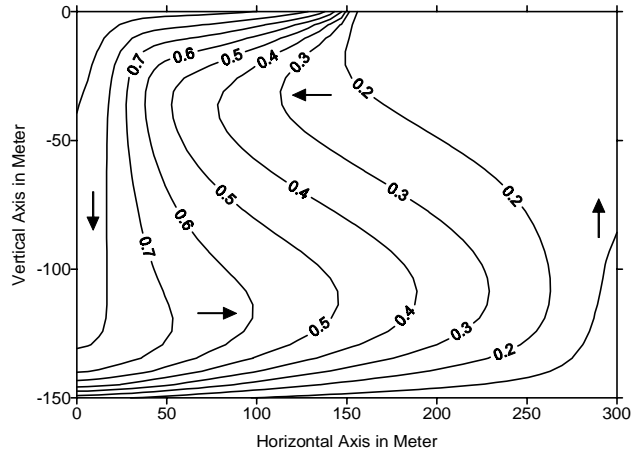


Figure 4. Steady state brine mass fraction at $y = 3$ m in three-dimensional case DEP1F

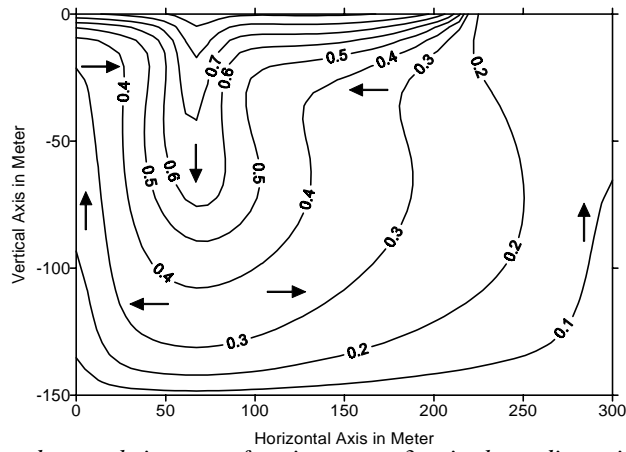


Figure 5. Steady state brine mass fraction at $y = 3$ m in three-dimensional case DEP2F

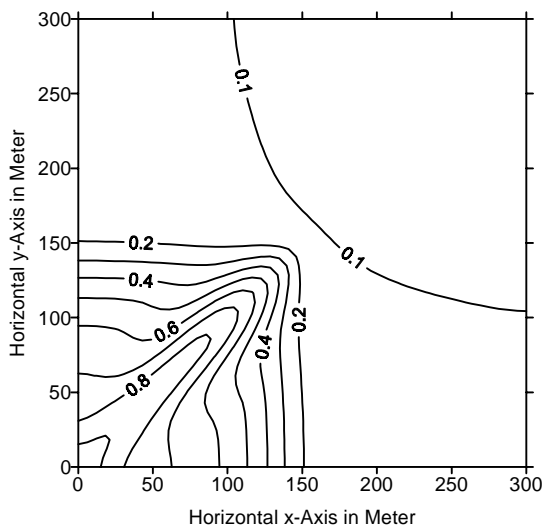


Figure 6. Steady state brine mass fraction at $z = -12.5$ m in three-dimensional case DEP1F

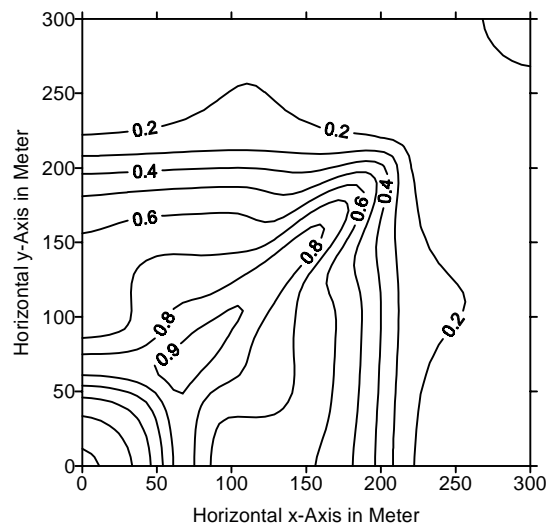


Figure 7. Steady state brine mass fraction at $z = -12.5$ m in three-dimensional case DEP2F

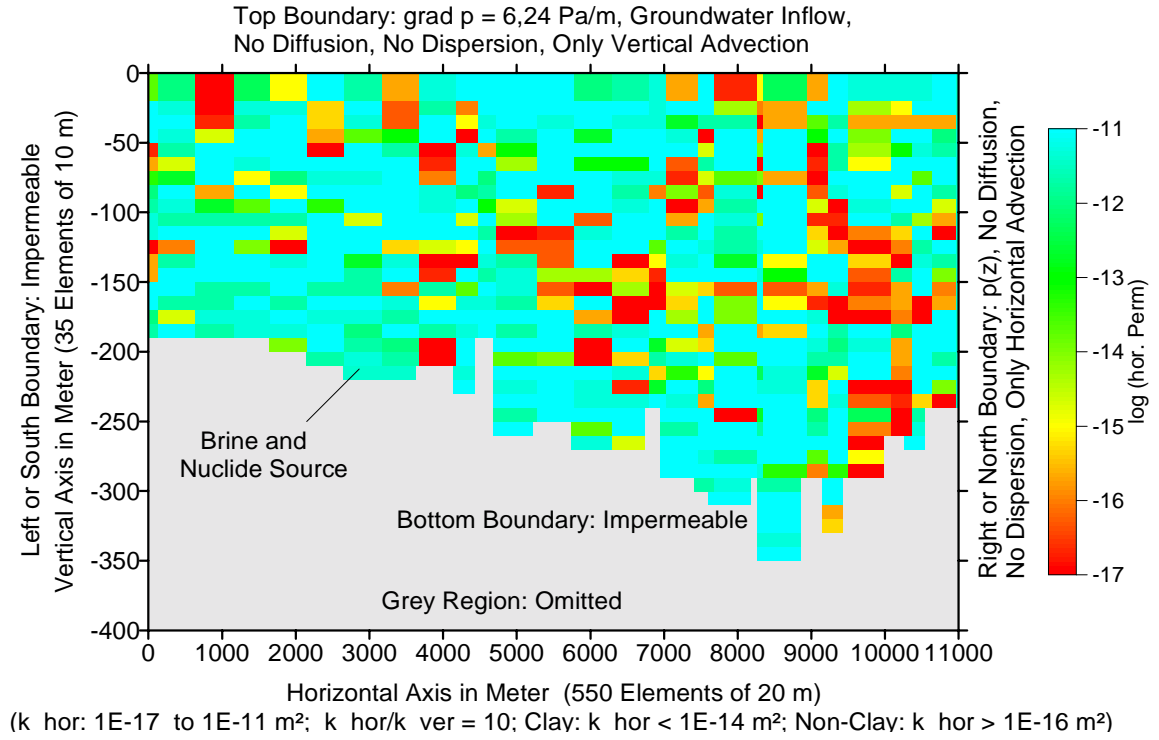


Figure 8. Distribution of horizontal permeability in a two-dimensional model

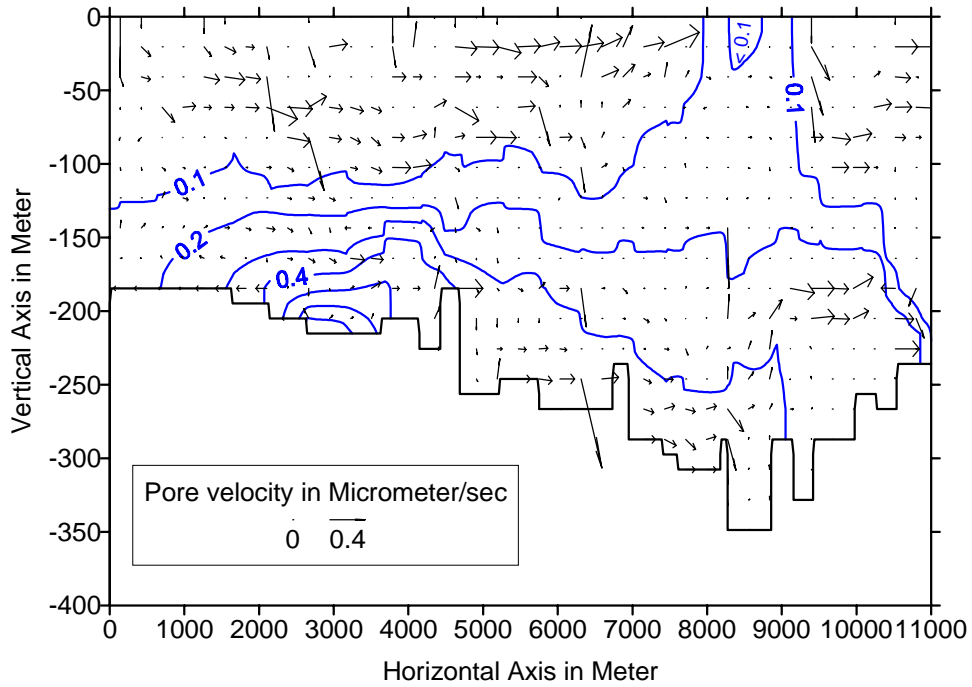


Figure 9. Steady state brine mass fraction and pore velocity in Case GP1

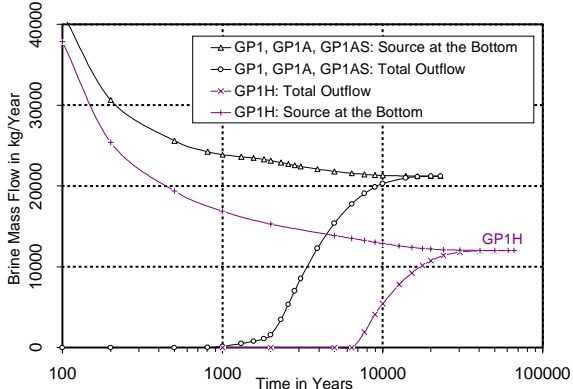


Figure 10: Brine Source at the Bottom and Total Outflow at the Boundaries

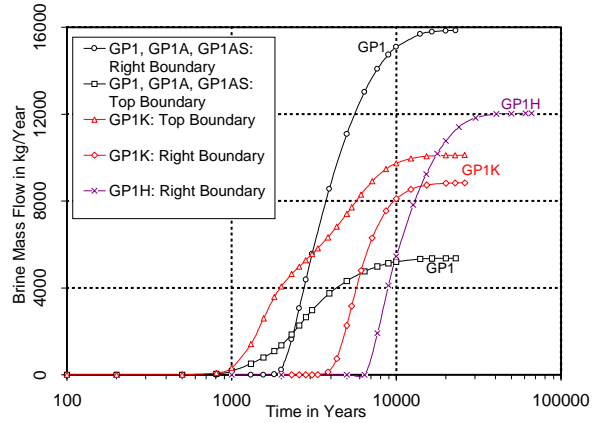


Figure 11: Brine Mass Outflow at the Boundaries

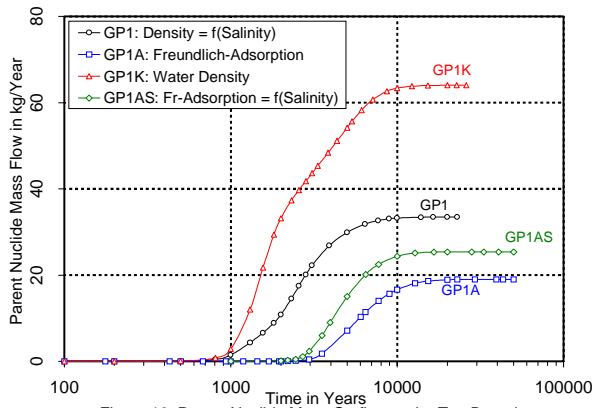


Figure 12: Parent Nuclide Mass Outflow at the Top Boundary

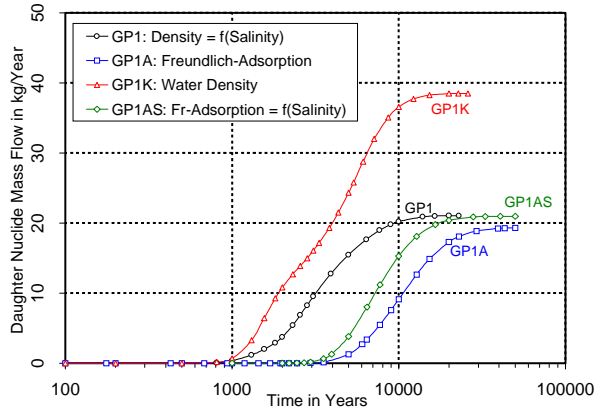


Figure 13: Daughter Nuclide Mass Outflow at the Top Boundary

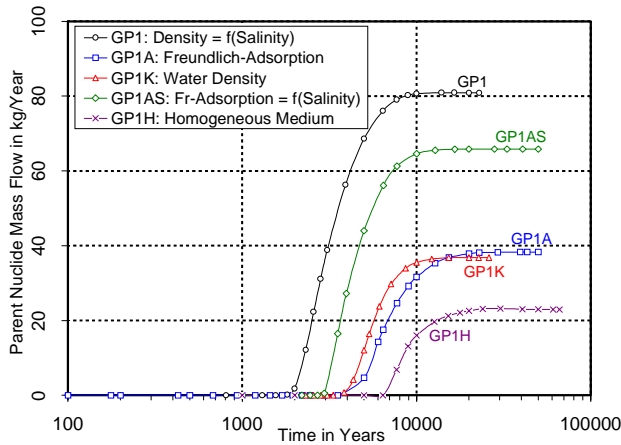


Figure 14: Parent Nuclide Mass Outflow at the Right Boundary

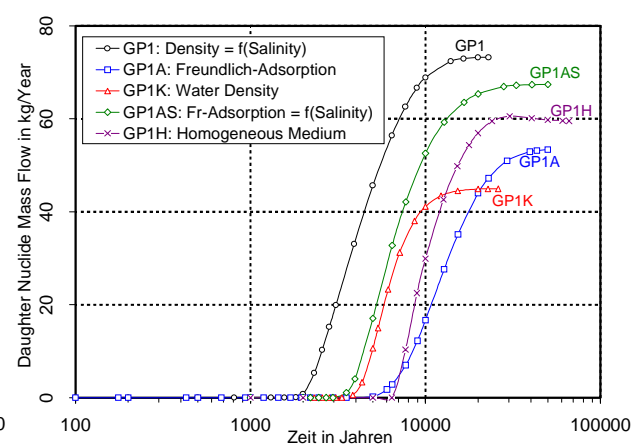


Figure 15: Daughter Nuclide Mass Outflow at the Right Boundary